Applied Catalysis B: Environmental 307 (2022) 121139

Contents lists available at ScienceDirect

Applied Catalysis B: Environmental

journal homepage: www.elsevier.com/locate/apcatb

A carbon-negative route for sustainable production of aromatics from biomass-derived aqueous oxygenates

Yehong Wang [a,b,1], Jiaxu Liu [c,1], Zhitong Zhao [d,1], Qiang Guo [a], Qike Jiang [a], Ning He [c], Feng Wang [a,*]

[a] State Key Laboratory of Catalysis, Dalian National Laboratory for Clean Energy, Dalian Institute of Chemical Physics, Chinese Academy of Sciences, 457 Zhongshan Road, Dalian 116023, PR China
[b] University of Chinese Academy of Sciences, Beijing 100049, PR China
[c] State Key Laboratory of Fine Chemicals and School of Chemical Engineering, Dalian University of Technology, No. 2 Linggong Road, Dalian 116024, PR China
[d] College of Chemistry and Chemical Engineering, Taiyuan University of Technology, Taiyuan 030024, Shanxi, PR China

ARTICLE INFO

Keywords:
Catalytic biomass conversion
Aromatization
Carbon-negative
Lewis and Brönsted acid catalysis

ABSTRACT

Sustainable technologies and efficient process design in chemical synthesis are in great demand for achieving a low-carbon society. Here, a sustainable approach for producing aromatics is designed via a biomass-derived carbon-negative route. A target aromatic yield of up to 50% was achieved using an industrial aqueous oxygenate mixture as the feedstocks. Such high performance is ascribed to the Zn modified ZSM-5 zeolites, which were proved to introduce synergistic catalysis involving Lewis acid sites and Brönsted acid sites, and were essential to aromatize these oxygenates efficiently. This approach provides a promising route for converting biomass-derived complex mixtures to valuable chemicals toward the carbon-neutral goal.

1. Introduction

Building environmentally benign and sustainable roadmaps toward low-carbon societies is a global consensus and prospect. The global scientific community is at the prospect of reaching a CO_2 emission peak before 2035 and achieving carbon-neutral within the next 30–40 years [1–4]. Strict CO_2 emission policies are increasingly being implemented and put tremendous pressure on chemical industries, where one of the pivotal branches is the production of aromatics, particularly benzene (B), toluene (T), ethylbenzene (E), and xylene (X), through catalytic reforming of naphtha [5,6]. Althogh the aromatization of alkanes, olefins, alcohols, and syngas enables alternative fossil routes for producing aromatics [7–12], the escalating consumption of aromatics and strict policies call for synthetic breakthroughs in the merits of green and low-carbon footprint. One promising approach is to convert renewable and sustainable biomass to aromatics. Industrial fermentation processes facilitate bio-transformation of polysaccharides and other biomass wastes, which involve interconnected structures and high oxygen content (35–45%), to small oxygenates mixtures [13,14]. Subsequent conversion of these abundant fermentation broths to aromatics shows excellent potential. However, controlling the selectivity with high conversion is yet a significant challenge.

Acetone-butanol-ethanol (ABE) fermentation was the second-largest industrial bioprocess which produced primarily bio-butanol from biomass. However, the oxygenates complex induced high purification costs, resulting in incompetent applications. In the recent decade, direct conversion of ABE mixture to high-valuable fuels and chemicals received a great amount of attention from many research groups [15,16]. Via a combined process involving metal-catalyzed dehydrogenation/ hydrogenation and base-catalyzed Aldol condensation, the ABE mixture was transformed to ketones or alkanes [15,16]. However, these processes generated various intermediate aldehydes that were mixed with acetone and not stable under the reaction conditions. Random condensation took place among these intermediates to produce ketone or alkane mixtures with a broad distribution of carbon species. In 2018, we developed a new strategy for the selective transformation of aqueous ABE mixture to 4-heptanone. In this catalytic system, the random condensation of aldehydes was partially inhibited due to the activation of H_2O, leading the oxidative condensation of aldehydes to generate 4-heptanone [17]. Henceforth, controlling or even inhibiting the

* Corresponding author.
E-mail address: wangfeng@dicp.ac.cn (F. Wang).
[1] These authors contributed equally to this work.

https://doi.org/10.1016/j.apcatb.2022.121139
Received 20 September 2021; Received in revised form 31 December 2021; Accepted 21 January 2022
Available online 25 January 2022

formation of active aldehyde intermediates is essential to the selective conversion of ABE mixture to high-valuable chemicals. However, few relevant processes had yet been developed. We propose a rational design and synthesis of preferable acidic catalysts, which will lead the ABE conversion to start with the deoxygenation for generating hydrocarbons. And the subsequent coupling via an aromatization process will enable the selective conversion of aqueous ABE mixture to aromatics.

MFI-typed zeolites as typical acidic catalysts have been widely used in catalytic biomass refinery and fossil-derived aromatization reactions [18–22]. Unlike the fossil routes for aromatization, the aromatization of aqueous ABE mixture is not limited to the aromatization of olefins but also the deoxygenation of oxygenates. It requires a rational design and preparation of acidic zeolites with appropriate acid types (Brönsted and Lewis acid sites, denoted as BAS and LAS herein) and distributions [23–25]. Generally, the selective generation of aromatics could be enhanced by introducing metals to ZSM-5 [26]. In particular, Zn and Ga were known as efficient Lewis acid sites in modified ZSM-5, providing dehydrogenation sites for dehydrocyclization and suppressing hydrogen transfer reactions leading to inert alkanes [20,27]. Thus, the design and synthesis of preferable acidic catalysts to balance the deoxygenation and aromatization are essential for the selective conversion of aqueous ABE oxygenates mixture.

In this work, we achieved the selective conversion of biomass-derived aqueous ABE mixture to aromatics over Zn modified ZSM-5 catalyst. The liquid yield reaches 58% with 86% BTEX selectivity in liquid, which is comparable with that in the conventional catalytic reforming (55% BTEX yield) and superior to other biomass-derived routes, such as catalytic pyrolysis (< 30% BTEX yield) [5,22,28,29]. Under the investigated conditions, we revealed that the reaction pathways were attributed to the synergistic catalysis by both Lewis acid and Brönsted acid. Life cycle assessment suggests that greenhouse gas emissions of our proposed process can be negative. This process provides a new biomass-derived route for the selective conversion of aqueous oxygenate mixture to aromatics, not only relieving the carbon dependence on fossil resource but also reducing the emission of CO_2.

2. Experimental section

2.1. Preparation of catalysts

HZSM-5, HY and H-MOR zeolites with various Si/Al were purchased from Nankai Catalysts Company, China. The metals were introduced into HZSM-5 zeolites by wet impregnation. Typically, 1.0 g HZSM-5 was dispersed in an aqueous solution of $Zn(NO_3)_2{\cdot}6H_2O$ and stirred slowly for 20 h. The Zn containing was tuned carefully according to the Zn loading amount (1 wt%∼5 wt%). Then the slurry was dried at 100 °C by evaporation and calcined at 550 °C in air for 4 h. The same preparation procedure was employed for other metal introduction (Ga, Yb, and Ce, respectively) to HZSM-5 catalysts with 2% metal loading amount based on the weight. They were denoted as 2Ga/HZ5, 2Yb/HZ5, and 2Ce/HZ5, respectively.

2.2. Catalyst characterizations

Powder X-ray diffraction patterns were obtained with a Rigaku D/Max 2500/PC diffractometer, using Cu-Ka radiation at 40 kV and 20 mA. Continuous scans were collected in the 2θ range of 10°–80°, at a step rate of $2^{\circ}{\cdot}min^{-1}$. The Brunauer-Emmett Teller (BET) surface area and pore volume were measured by nitrogen adsorption-desorption using a Quantachrome Autosorb-1. X-ray photoelectron spectroscopy (XPS) analysis was performed using an ESCALAB250Xi (Thermo, USA), with an Al-Kα (1486.6 eV) excitation source. *In situ* DB-FTIR spectrometry was used to study the surface reaction processes and the structure of the adsorbents and intermediates on HZ5 and the Zn modified HZ5 catalysts under real reaction conditions. The as-calcined catalysts were used directly as the tested samples. The sample was pressed into self-supporting thin wafers (1 cm^2), which were placed in the sample beam, while the reference beam was vacant. The sample was activated in the dual-beam IR reactor cell at 410 °C for 4 h under vacuum (10^{-3} Pa), and spectra were recorded at a resolution of 4 cm^{-1} with 64 scans in the region of 4000–1000 cm^{-1}. The intensities of the reference and sample beams were adjusted to the same level. The effluent from the IR reactor cell was analyzed using a quadrupole mass spectrometer (Omnistar, 1–200 amu, QMS 200). The ABE aromatization was carried out at the temperature of 400 °C under the constant pressure of 0.1 MPa. ABE was fed continuously by a nitrogen carrier gas (10 mL min^{-1}) at saturated vapor pressure. The spectra were obtained by subtracting the background spectrum (obtained from the sample-free reference beam) from the measured sample spectra.

2.3. Evaluation of catalytic performance

The aromatization reactions were conducted in the fixed-bed reactor. The zeolites were pressed into pellet under 10 MPa and crushed to 40–60 mesh small particles. 1.0 g or 2.0 g of catalyst was then loaded into a vertical quartz reactor heated by an electric furnace. The internal diameter of the reactor is 7 mm. Aqueous ABE mixture feedstocks were fed into the reactor by a pump and N_2 was used as the carrier gas (9 $mL{\cdot}min^{-1}$). The aqueous ABE mixture is applied as the feedstock with an Acetone: Butanol: ethanol mass ratio as 3:6:1 to simulate fermentation by Clostridium acetobutylicum). The water content is varying from 0% to 40% based on weight. The reactions were conducted at 400 °C unless additional instruction. Products and unreacted feedstock were collected in a cold trap and were analyzed by gas chromatography (GC) with benzotrifluoride as the internal standard.

2.4. Life cycle assessment (LCA)

Life cycle assessment (LCA) is used to evaluate primary fossil energy (PFE) depletion and greenhouse gas (GHG) emissions of this work. LCA is an effective tool to evaluate environmental benefits, which is defined as “compilation and evaluation of the inputs, outputs and potential environmental impacts of a product system throughout its life cycle” [30]. The functional unit is defined as 1 metric ton of xylene. The system boundary covers PFE depletion and GHG emissions for the corn stover collection, transport, ABE extraction from corn stover fermentation, and conversion of ABE into aromatic hydrocarbon, and all upstream of required materials and utilities. The details are shown in Supporting Information.

3. Results and discussion

3.1. Characterizations of HZ5 and Zn modified HZ5 catalysts

HZSM-5 zeolite (SiO_2/Al_2O_3 is 46, denoted as HZ5 (46) herein) was purchased and applied as typical Brönsted acid in this catalytic system. Zinc, which always behaves as the Lewis acidic site in zeolites, was introduced to HZ5 (46) by impregnation for tuning the acid properties of HZ5 (46). The Zn modified HZ5 catalysts were denoted as XZn/HZ5 and X stands for the loading amount of Zn based on weight. All these catalysts were typical MFI structure, where no diffraction peaks associated with ZnO phase was found after the introduction of Zn species from the XRD patterns (Fig. S1). Similarly, the introduction of Zn species did not decrease the specific area or pore volume (Fig. S2 and Table S1). HAADF-STEM (Fig. 1) images show that Zn species was highly dispersed in 2Zn/HZ5 (46) (Figs. 2a and S3), while Zn species in 5Zn-HZ5 agglomerated to particles (Fig. 2b). The presence of highly dispersed Zn clusters on 2Zn/HZ5 was also verified by the UV-Vis absorption spectra due to the presence of the absorption band located at ∼270 nm (Fig. S4). The cluster size is generally smaller than 1.0 nm [31]. XPS was applied to study the chemical states of Zn species. The binding energy at 1021.73 eV (Zn 2 P) in 2Zn/HZ5 catalyst is attributed to highly

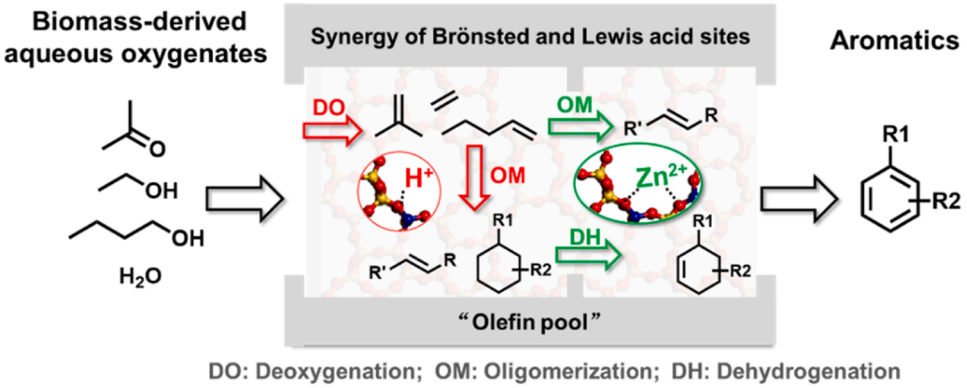

Fig. 1. The selective conversion of biomass-derived aqueous ABE mixture to aromatics over Zn/HZSM-5 catalyst by the synergistic catalysis of BAS and LAS.

dispersed Zn species (Fig. 2c). For comparison, a lower binding energy at 1021.08 eV appears in 5Zn/HZ5 due to the formation of ZnO particles (Fig. 2d), which is in a good agreement with the HAADF-STEM results. Considering the crucial roles of acid properties in aromatization, the following studies were performed carefully. Firstly, Pyridine-IR was applied to investigate the acid types (BAS and LAS) (Fig. 2e–g) (Table S2). For HZ5, a remarkable band at 1546 cm^{-1} which is assigned with BAS stands even after being evacuated at 450 °C, indicating the strong strength of these BAS. The introduction of Zn to HZ5 leads to a decrease of BAS while increasing LAS (1445 cm^{-1}~1455 cm^{-1}), indicating the Zn species located on BAS. Based on the results of Pyridine-IR, the concentration of BAS and LAS were calculated (Fig. 2h). For HZ5, the concentration of BAS and LAS is ~0.32 mmol/mg and 0.01 mmol/mg, respectively. The ratio of BAS to LAS (denoted as B/L) is ~32, suggesting that the surface is majorly covered by BAS. The B/L of 2Zn/HZ5 decreases to 1.6, suggesting the co-existence of BAS and LAS. The B/L continues to decrease to 0.29 with increasing the Zn loading amount to 5 wt%, which indicates that the LAS dominates in 5Zn/HZ5. These results reveal that the concentrations and ratio of LAS to BAS has been successfully tuned. Three typical acidic zeolites were obtained: BAS for HZ5, co-existence of BAS and LAS for 2Zn/HZ5, while majorly LAS for 5Zn/HZ5.

3.2. *Catalytic performances of HZ5 and Zn modified HZ5 catalysts in the aromatization of aqueous ABE mixture*

HZ5 and Zn/HZ5 catalysts were applied in the aromatization of aqueous ABE mixture (A: B: E = 3:6:1 based on weight, H_2O: 21 wt%) at 400 °C under atmospheric pressure. The results were shown in Fig. 3(a). Based on the results, the conversion for all catalysts were achieved > 99% with carbon balance > 86%. When HZ5 was used as catalyst, a large amount of gas (including CO, CO_2, CH_4, and C_2-C_4 alkanes and olefins) was obtained with 57% gas yield. The liquid yield is ~35% consisting with 32% aromatics and other C9 + by-products such as naphthalene. The yield of BTEX in liquid is only about 30%. The liquid yield is significantly improved to 54% with 51% aromatics yield after 2 wt% Zn was introduced, and the yield of BTEX achieved 48%. Further introducing the Zn to 5 wt% (5Zn/HZ5) resulted in the liquid yield decreasing to 41% with 31% BTEX yield. Fig. 3(b) shows the distributions of products in the liquid phase, which is especially crucial for the separation. The liquid product consisted of 90% aromatics and 10% C9 + products over HZ5. The BTEX selectivity in liquid is ~86%. When 5Zn/HZ5 was used as catalyst, up to twice C9 + products (~21%) were generated. The BTEX selectivity in liquid decreased to 77%. In contrast, the highest aromatics selectivity (94%) and BTEX selectivity (89%) were obtained over 2Zn/HZ5, suggesting its excellent catalytic performance. According to the results of Pyridine-IR, synergistic catalysis of BAS and LAS in 2Zn/HZ5 might contribute to its high catalytic activity in the aromatization of aqueous ABE mixture. Great effects are also made to optimize both the catalysts and reaction conditions. Compared with HZ5 (46), either increasing or decreasing the ratio of SiO_2 to Al_2O_3 would decrease the selectivity of BTEX (Table S3, entries 1–3). We also attempt to introduce other metals to modify HZ5, such as Ga, Yb or Ce instead of Zn, but the BTEX selectivity and liquid yield were not improved significantly (Table S3, entries 7–9). It was further confirmed that the appropriate acidic site is essential to this aromatization reaction. When other zeolites that did not belong to MFI-typed zeolites (HY: 12 member ring, 0.74*0.74 nm or HMOR: 12 member, 0.70 *0.65 and 8 member ring, 0.57 *0.26 nm) were applied in this reaction, no aromatics were obtained and only low carbon olefins (C2-C4) were observed (Table S4). This result reveals the crucial role of shape-selectivity in the aromatization of the aqueous ABE mixture. MFI-typed zeolites, particularly ZSM-5, are medium-pore zeolites with interconnected 10-membered straight and sinusoidal pores. The straight channel has dimensions of 0.53 * 0.56 nm, while the sinusoidal channel has dimensions of 0.55 * 0.51 nm, which permit the formation and transportation of light aromatics (~ 0.55 nm). The shape-selectivity is further verified by the fact that HZ5 (46) loses its aromatization activity after milling due to the collapse of micro-pores (Table S5). On the basis of excellent catalytic activity of 2Zn/HZ5, the effects of reaction conditions, such as reaction temperature, WHSV and contact time on the conversion and products distribution were then investigated (Fig. 3c). As temperature increases or contact time shortens, the liquid yield decreases although the selectivity of BTEX is slightly improved. Increasing the WHSV from 1.25 h^{-1} to 2.5 h^{-1} has a positive effect, and a high liquid yield (58%) and BTEX selectivity (86%) is obtained. This result is comparable to that of aromatization via conventional petroleum or coal routes, suggesting the potential application in industry.

Water is an unavoidable product during fermentation. The water content in the fermentation broth is generally higher than 97% at the initial. Then it could be sharply decreased to ~40% via distillation. Further separation should be proceeded by rectification to obtain three major compounds, which is an undesirable process with high energy consumption. Thus, to convert the aqueous ABE mixture directly is essential to widely apply the biomass-derived fermentation broth. Here, the effect of water with a content ranging from 0% to 40% on the aromatization of the aqueous ABE mixture was investigated carefully. Liquid yield of 41% with a 69% BTEX selectivity and ~30% C9 + selectivity is obtained when anhydric ABE mixture was used as the feedstocks (Fig. 4a–b). The addition of water into the ABE mixture positively affects the liquid yield, which is improved to 51% even with 9 wt% water addition. Neither the liquid yield nor the BTEX selectivity is improved when continuing to increase water content (Fig. 4b). However, higher water content could inhibit the formation of coke. (Fig. S5). The effect of water on the removal of carbon deposition was also found in the aromatization of ethylene and other reactions, such as propane dehydrogenation and methanol-to-olefins [32–36]. The coke is generally suppressed by feeding water, either due to the reaction

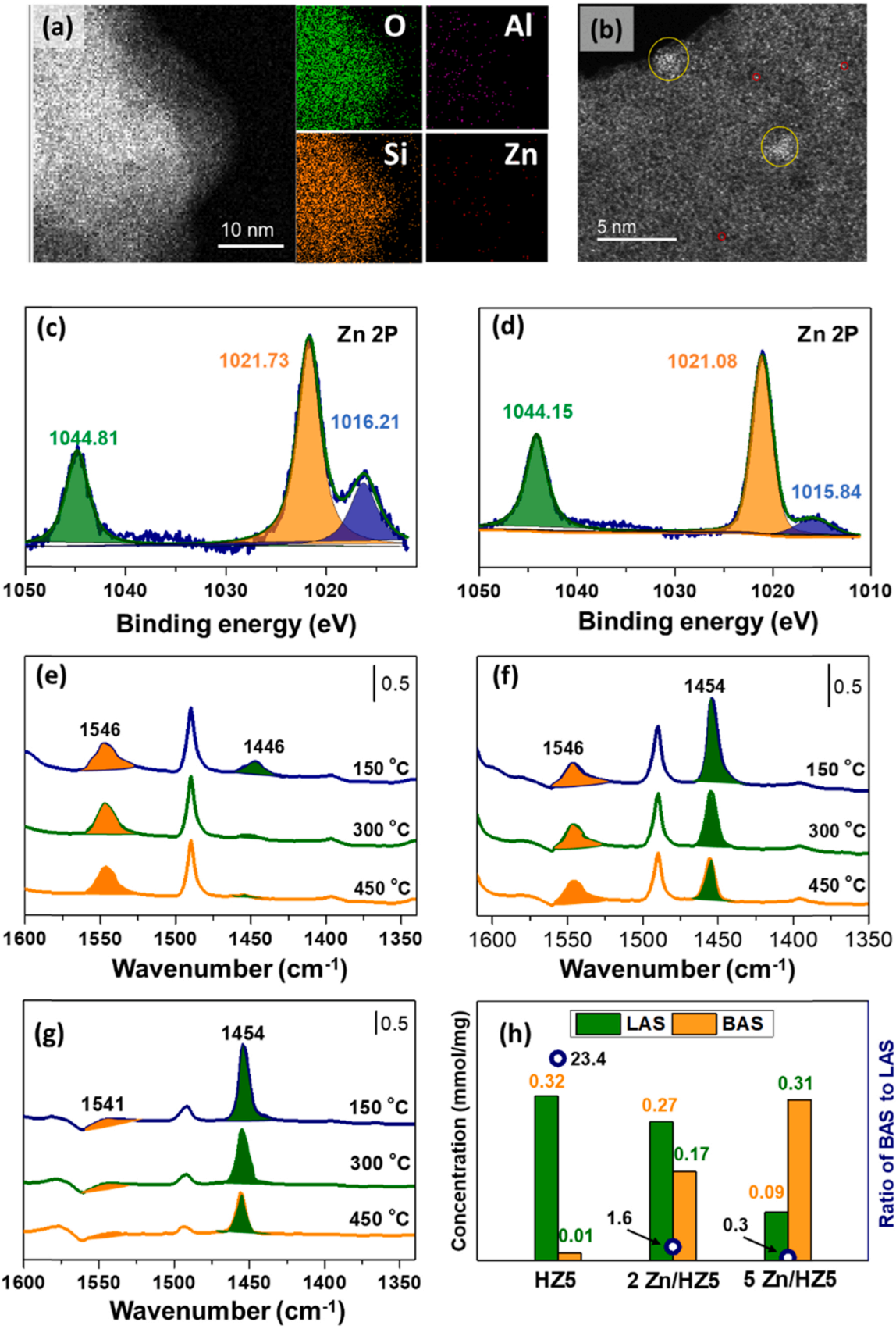

Fig. 2. Characterizations of HZ5 and Zn/HZ5 catalysts. (a) HAADF-mapping results of (a) 2 Zn/HZ5, (b) HAADF-STEM images of 5Zn/HZ5; core-level Zn 2P XPS spectra of (c) 2Zn/HZ5, (d) 5Zn/HZ5, and Pyridine-IR spectra of (e) HZ5, (f) 2Zn/HZ5, and (g) 5Zn/HZ5, (h) acid concentration and the ratio of BAS to LAS for HZ5 and Zn/HZ5, respectively.

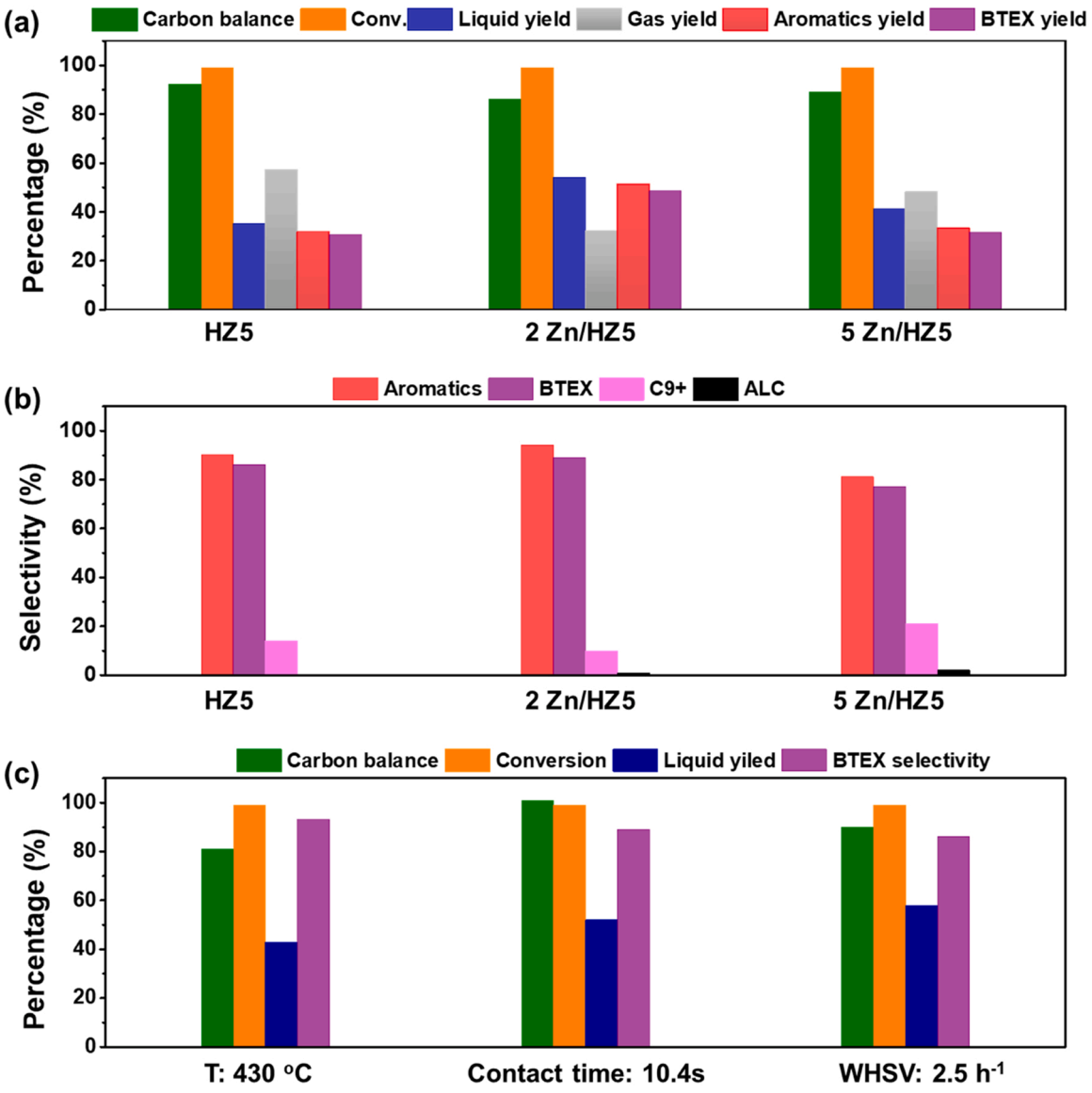

Fig. 3. The conversion of aqueous ABE mixture over HZ5 and Zn/HZ5 catalysts under different reaction conditions. (a) The catalytic performance of HZ5 and Zn/HZ5 catalysts. Reaction conditions: catalyst (2 g, 40–60 mesh), N_2 as carrier gas (9 mL·min^{-1}), 400 °C, WHSV = 1.25 h^{-1}, contact time 12 s. ABE solution was used as feedstock, where the A: B: E weight ratio was 3:6:1, H_2O: 21 wt%. (b) The distribution of products in liquid. (c) The effect of reaction conditions. The reaction conditions are the same as those above except for extra detail. Abbreviations: Conv., conversion; ALC, aliphatic hydrocarbons; C9+, hydrocarbons with higher than 9 carbon numbers.

between carbon and water to release CO and H_2, or postponed condensation and polymerization from aromatics to polyaromatic hydrocarbons which is one of coke precursors. In this work, trace CO was detected for the reaction with or without water addition. In contrast, from a comparison of liquid products distribution, the selectivity of C9 + hydrocarbons particularly the polyaromatic hydrocarbons decreased significantly (30% without water *VS* 10% with water) during the ABE mixture aromatization in the presence of water while with an increase of aromatics selectivity (69% without water *VS* 88% with water). It was proposed that the suppression of coke deposition by water addition is probably due to the partial inhibition in the condensation and polymerization from aromatics to polyaromatic hydrocarbons.

A continuous reaction for the conversion of aqueous ABE mixture (A: B: E = 3:6:1, water content: 21 wt%) to produce BTEX was then tested over 2Zn/HZ5 catalyst. The cold-trapped liquid phase naturally separates into two layers, which could be easily separated in a separatory funnel. Organic phase contains aliphatic olefins, BTEX, C9 + products, while the aqueous phase majorly contains water, occasionally trace amounts of unreacted acetone. In the initial 5 h, ~45% liquid yield was achieved with ~80% BTEX selectivity in liquid product. Then, the liquid yield decreases from 45% to 24%. The result of Pyridine-IR on spent 2Zn/HZ5 indicates that both LAS and BAS concentrations are decreased significantly. We assume that the blockage of acid sites by coke was probably the key factor for the deactivation. The coke on the catalyst can be removed by calcination. After two reaction-regeneration-reaction cycles, the BTEX selectivity still keeps at 90%, but a decrease in liquid yield (~30%) (Fig. 4c). Thus, further research focus on efficient Zn/HZ5 catalyst with excellent stability is undergoing. It should be noted that the distribution of BTEX obtained here is similar to that of the gasoline cracking, suggesting a potential industrial use via the current separation processes (Fig. 4d).

3.3. Proposed reaction mechanism

A combination of acidic properties characterization and catalytic activity for 2Zn/HZ5 inspired us to deduce the key role of synergistic

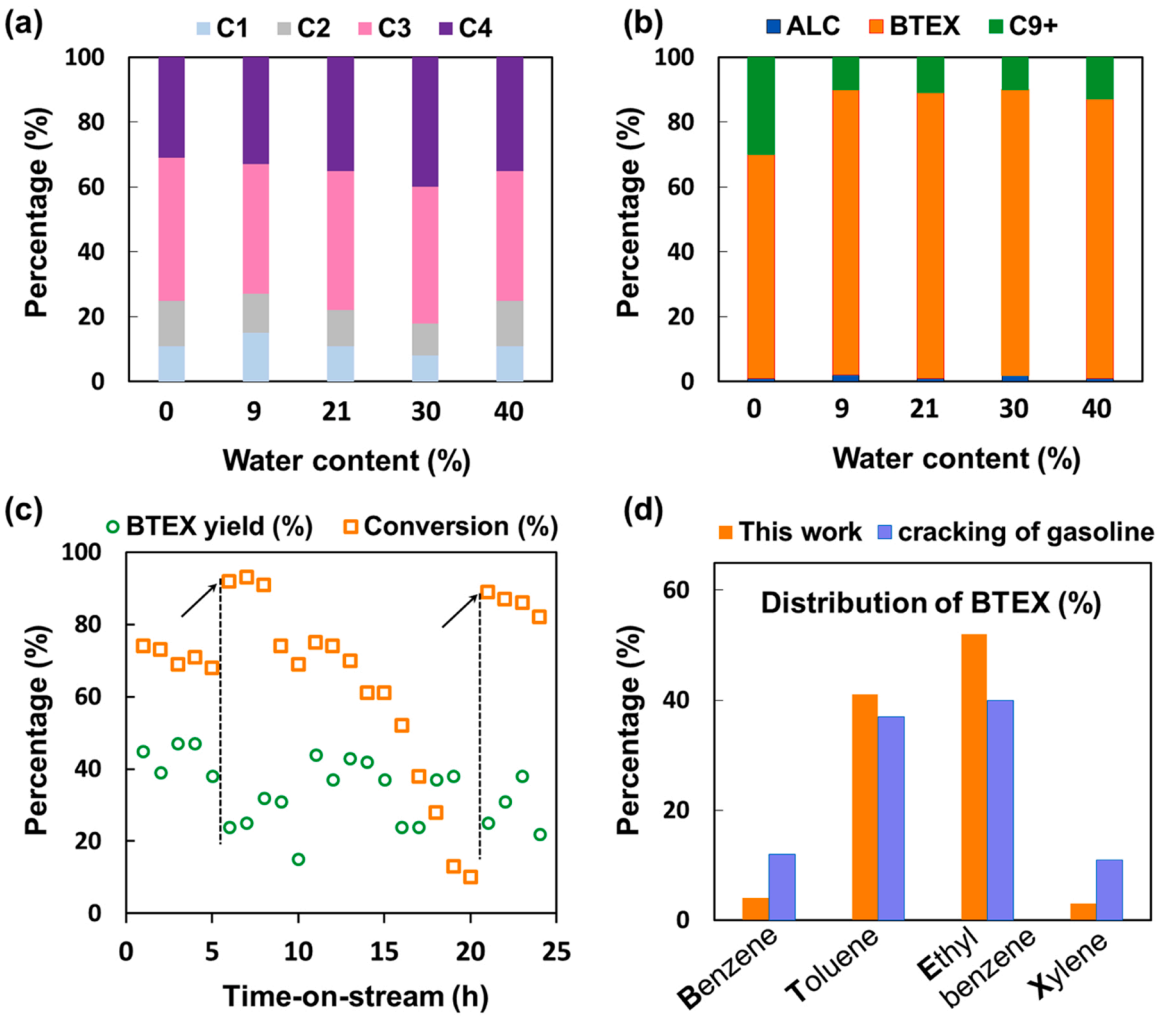

Fig. 4. The influence of water content in the aqueous ABE mixture feedstock. (a) The gas yield and the distribution of gas products. (b) The liquid yield and the distribution of liquid products. Reaction conditions: catalyst (2 g, 40–60 mesh), N_2 as carrier gas (9 mL·min^{-1}), 420 °C, WHSV = 1.25 h^{-1}. The A: B: E weight ratio was 3:6:1, water 21 wt%. (c) Catalyst life test. Catalyst (2Zn/HZ5, 2 g, 40–60 mesh), N_2 as carrier gas (5 mL·min^{-1}), 410 °C, WHSV= 2.5 h^{-1}. ABE solution was feedstock with A: B: E as 3: 6: 1, and 21 wt% water content. Arrow respects the regeneration of catalyst by calcination in air at 600 °C for 4 h. (d) Comparison of BTEX distribution obtained from our catalytic system and gasoline cracking.

catalysis of BAS and LAS. *In situ* dual–beam FTIR (DB-FTIR) was applied to evaluate the catalysis of BAS and LAS by tracking the reaction intermediates during this aromatization process by deducting the reference signals to exclude the strong heat irradiation (Fig. S6) [37,38]. Typically, the conversion of ABE with weight ratio 3:6:1 was tracked by *in situ* DB-FTIR spectrometer at 400 °C at atmospheric pressure. A series of bands located at 1612, 1583, 1563, 1505 and 1445 cm^{-1} were observed in the spectra (Fig. 5a). To assign these bands clearly, *in situ* DB-FTIR was conducted with acetone, butanol, and ethanol acting as probe molecules, respectively. Fig. 5b shows the *in situ* DB-FTIR spectra of acetone aromatization on 2Zn/HZ5 (46), while that on HZ5 (46) and 5Zn/HZ5 (46) were also conducted for comparison (Fig. S7). The attribution for various bands in details is shown in Table S6. The intermediate species observed could be divided into five groups: (1) adsorbed acetone; (2) α, β-acetone-C═C, generated from the self-coupling of acetone; (3) adsorbed R-C═C- linked to Zn, which was considered as the precursor of aromatics; and (4) the adsorbed aromatics; (5) adsorbed carboxylic acid. The band located at 1738 cm^{-1} was assigned to the *ν*(C═O) of adsorbed acetone, indicating the activation of acetone. The bands located at 1666–1658 cm^{-1} and 1638 cm^{-1} were assigned to *ν*(C═O) of α, β-acetone–C═C-R species. The band located at 1608 cm^{-1} was assigned to adsorbed carboxylic acid. The formation of these species was also verified by the products distribution of acetone conversion at a lower temperature (300 °C) (Fig. S8). Mesityl oxide, isobutylene and acetic acid were generated via self-condensation and scission of acetone. The bands located at 1583–1587 cm^{-1} were assigned to the *ν*(C═C) of –C═C–R linked to Zn sites, and these species were considered as the precursor for the aromatics production via cyclization and dehydrogenation. The bands located at 1534 and 1508 cm^{-1} were assigned to the stretching vibration of benzene ring, indicating the aromatics adsorbed on the surface of catalyst. In addition, the presence of the bands at 1445 and 1365 cm^{-1} were due to the –CH_2 or –CH_x species. It is noteworthy that the conversion of acetone on HZ5 is different from that on Zn modified HZ5 from the *in situ* DB-FTIR spectra. For HZ5, the adsorbed aromatics was observed but no band associated with R–C═C–. In contrast, –C═C– linked to Zn species were observed but no adsorbed aromatics on Zn/HZ5. Based on these results, the process for acetone aromatization is proposed as follows: mesityl oxide is generated from the self-coupling of acetone, and then cracked into isobutene and acetic acid; the generated isobutene acts as "initial olefin pool" and participates in the subsequent aromatization. It is noteworthy that the conversion of acetone on HZ5 is significantly different from that on Zn modified HZ5. For HZ5, the adsorbed aromatics was observed but no band associated with –C═C–. It suggests that BAS could catalyze the aromatization smoothly but with strong adsorption for aromatics, leading to the deactivation of the catalyst. In contrast, there was no

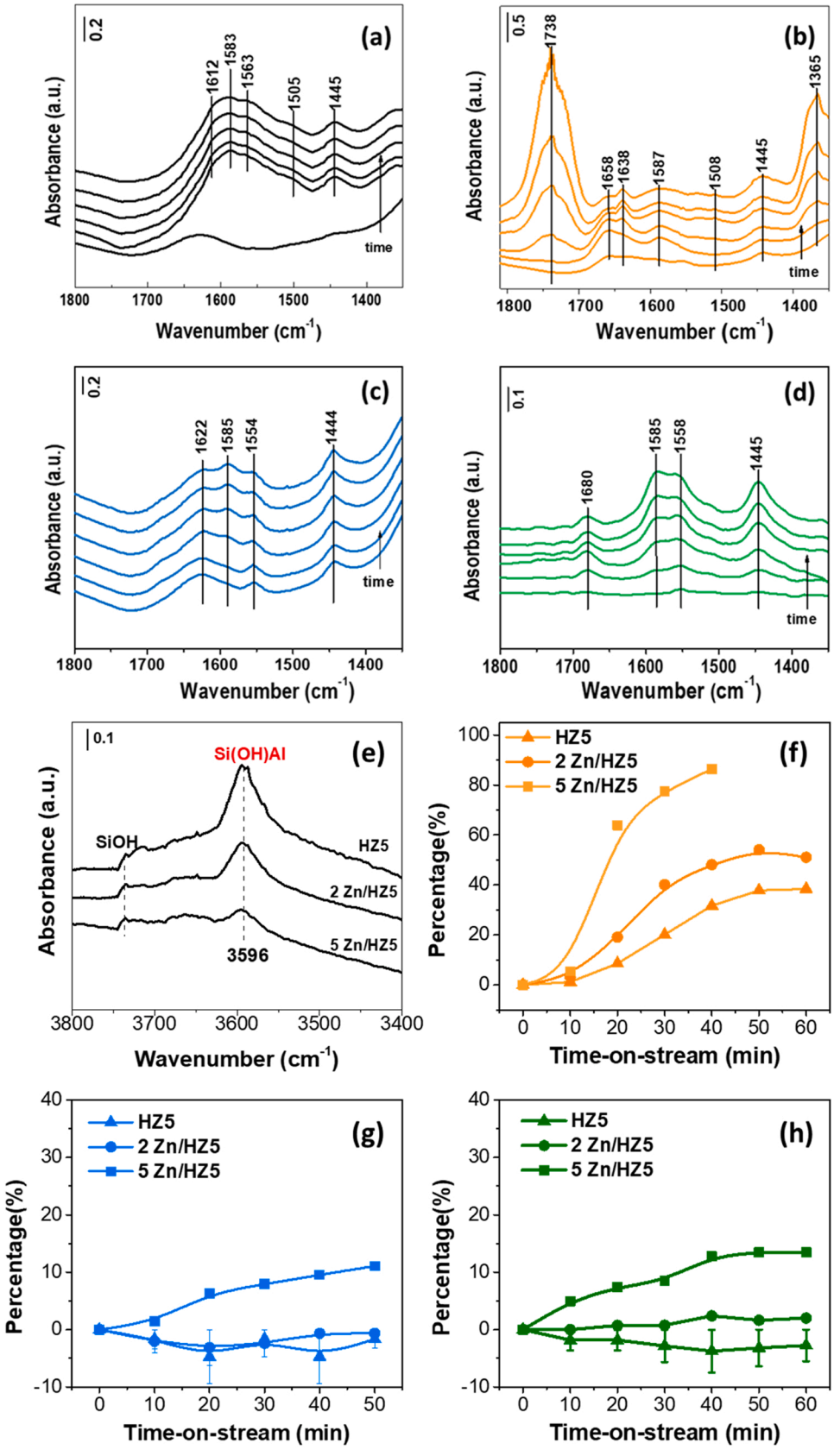

Fig. 5. The *in situ* DB-FT-IR spectra results. (a) Aromatization of ABE over 2Zn/HZ5, A: B: E = 3:6:1; (b) aromatization of acetone over 2Zn/HZ5; and (c) aromatization of ethanol over 2Zn/HZ5; (d) aromatization of butanol over 2Zn/HZ5; (e) the hydroxyl group assigned to BAS detected under reaction conditions; (f) the participation of BAS in acetone aromatization on HZ5 and Zn/HZ5; (g) the participation of BAS in ethanol aromatization on HZ5 and Zn/HZ5; (h) the participation of BAS in butanol aromatization on HZ5 and Zn/HZ5. The spectra were recorded for each 10 min.

adsorbed aromatics on Zn/HZ5, indicating that the addition of Zn sites enhanced the desorption of aromatics, leading to the high selectivity of aromatics. In particular, obvious bands assigned to the R-C═C-Zn were observed, which could be transformed to aromatics via oligomerization or/and cyclization and dehydrogenation catalyzed by LAS. The catalytic activity of LAS in dehydrogenation was verified by the DFT calculations. For the DFT calculations, H^+, Zn^{2+} and $(Zn\text{-}O\text{-}Zn)^{2+}$ were chosen as main active sites for HZ5, 2Zn/HZ5, and 5Zn/HZ5 catalysts, respectively. The dehydrogenation of cyclohexadiene, which was selected as the aromatic precursor, was calculated. The result reveals that the addition of Zn accelerated the C-H bond activation obviously and then to benzene via dehydrogenation (Fig. S9). Similarly, the reaction intermediates for the ethanol, butanol, or ABE mixture aromatization were detected and were majorly assigned to "olefin pool" species, indicating by the presence of the bands at 1554 cm^{-1}, 1585 cm^{-1} 1622 cm^{-1} and 1680 cm^{-1} which were assigned to the ν(C═C) of olefins (Fig. S10). The key role of LAS in the dehydrogenation of aromatics precursors was also verified by the reaction results. The addition of LAS (Zn sites), particularly with 2 wt% Zn, significantly improved the aromatics yield significantly. Although the liquid and aromatics yield was the lowest over HZ5, the conversion of aqueous ABE mixture achieved > 99% with 57% gas yield. It suggests the excellent catalytic performance of BAS in the deoxygenation to "olefin pool", although it is not so efficient in aromatization of olefins. The catalytic activity of BAS under the reaction conditions was confirmed by tracking the hydroxyl groups with *in situ* DB-IR (400 °C, atmospheric pressure). The absorbance at 3596 cm^{-1} for all samples corresponding to the hydroxyl group in Si(OH)Al, which acts as BAS. Its intensity decreased with the introduction of Zn, indicating the Zn species located on Brönsted acid sites, which is in good agreement with Pyridine-IR results (Fig. 5e). These results suggest the feasibility of tracking the evolution of BAS during aromatization. Then, the evolution of BAS during the aromatization was tracked by *in situ* DB-FTIR spectra at 400 °C over HZ5 and Zn/HZ5 (Fig. S11). The percentage of BAS participation was calculated as follows: $[(1\text{-}A(t)/A(t_0)] \times 100\%$; where A (t) is the integral area of band at 3596 cm^{-1} at a certain point of time, and the $A(t_0)$ is that at the beginning. About 38% of BAS was involved in the aromatization over HZ5 for acetone aromatization (Fig. 5f). Considering the total amounts of BAS from Pyridine-IR (0.39 mmol/g), there was ~0.142 mmol/g BAS participated in the reaction. For 2Zn/HZ5, a comparable BAS amount (0.138 mmol/g) were involved in the aromatization. It accounts for about 50% of total BAS over 2 Zn/HZ5 (Fig. 5g). For 5Zn/HZ5, the concentration of BAS involved in the aromatization of acetone was ~0.0863 mmol/g. However, ~86% of total BAS was reached over 5Zn/HZ5, which was due to the lower BAS total concentration (0.12 mmol/g) (Fig. 5h). These results suggest the aromatization of acetone could be catalyzed by BAS smoothly, and the catalytic activity follows the sequence: HZ5 ≈ 2Zn/HZ5 > 5Zn/HZ5. Similar *in situ* DB-FTIR was conducted for tracking the catalytic activity of BAS for ethanol or butanol aromatization. The BAS participated in the aromatization was less than 15% for either ethanol or butanol aromatization over all these three kinds of zeolite catalysts. The negative value in a range of < 5% probably came from the error during the integration of the peak area associated with Brönsted acid sites. These results reveal the crucial catalytic activity of BAS in deoxygenation of ABE, especially for acetone. The abovementioned results suggest that the synergistic catalysis of LAS and BAS, which contributed to the excellent catalytic activity of 2Zn/HZ5. More specifically, the catalytic deoxygenation of ABE to "olefin pool" is by BAS, while the formation of aromatics via dehydrogenation is by LAS.

In combination with the results of control experiments and *in situ* DB-FTIR, we proposed an "olefin pool" reaction process for aqueous ABE mixture to aromatics. Fig. 6 illustrates the reaction network for the aromatization of ABE, which could be summarized as follows: when the aromatization of aqueous ABE mixture is carried out, it could be generally divided into three steps: (i) the generation of "initial olefin pool": low carbon olefins were produced via deoxidization (BAS); the aqueous ABE mixture were smoothly transferred to olefins with a general high conversion even at low reaction temperature or short contact time; (ii) the generation of "secondary olefin pool": olefins with higher carbon numbers were produced via oligomerization (BAS+LAS) (iii) the aromatization of olefins via dehydrogenation (LAS). The aromatization of olefin particularly the dehydrocyclization is probably the rate-determining step. During this process, synergistic catalysis of LAS and BAS under reaction conditions is proposed, leading an excellent catalytic performance of 2Zn-HZ5 due to the co-existence and balance of BAS and LAS.

3.4. Economic and environmental analysis

The economic and environmental analysis was conducted to evaluate this biomass-derived route for the production of BTEX. A practical model of this work has been designed and simulated, employing corn stover as feedstock and aromatic hydrocarbon as targeted products, particularly xylene. The model involves ABE production process and conversion of ABE into aromatics. Furthermore, feedstock pretreatment, detoxification, hydrolysis, fermentation, ABE recovery, reaction from ABE to aromatics, and serials of separation units were contained (as shown in Fig. S12). Then rigorous material and energy balance inventory was obtained through steady-state simulation using Aspen plus based on current reaction conditions (Table S8). Techno-economic analysis and life cycle assessment were subsequently performed to examine economic and environmental feasibility. The results reveal that in our system, the minimum selling price (MSP) of the xylene in this work was estimated to 8044 CNY/t, which was 40% higher than the annual average price (5745 CNY/t) of xylene in China in 2019. To maximize the benefits of this work, a sensitivity analysis was conducted to evaluate the effects of 12 variables on the MSP, as shown in Fig. 7(a). From the results, toluene was the most sensitive factor to the MSP of xylene where a 10% difference leads to a −5.4% change. Followed by toluene, the FCI, corn stover, and electricity also cause more than 3.0% changes to the MSP of xylene. Other variables result in a less than 2.0% change. Thus the following researches should focus on improving revenue of toluene and

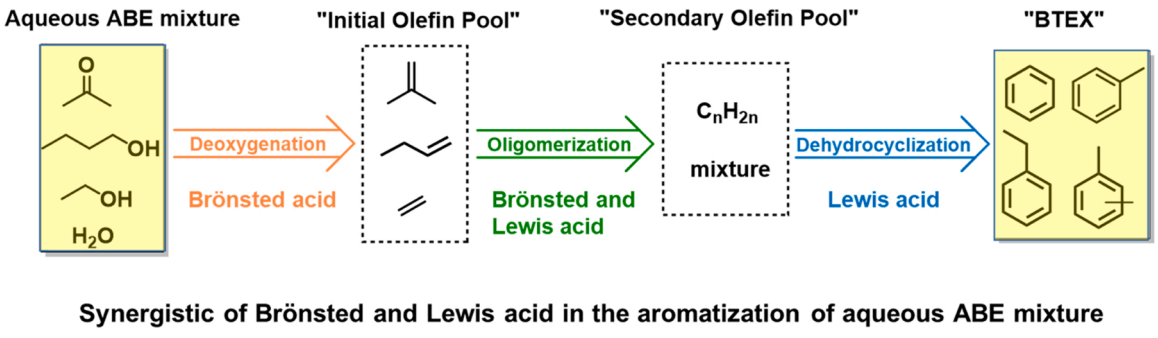

Fig. 6. A proposed mechanism based on the experimental results for the aromatization of aqueous ABE mixture to BTEX over Zn modified HZSM-5 catalyst.

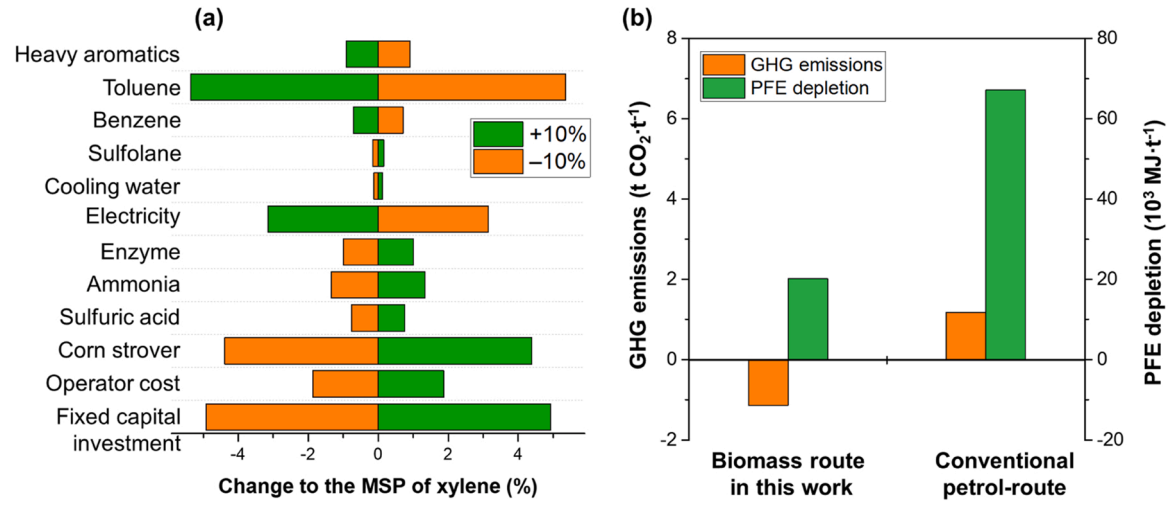

Fig. 7. (a) Sensitivity analysis for the MSP of p-xylene; (b) life cycle GHG emissions and PFE depletion of aromatics production via conventional petrol-route and biomass route in this work.

reducing consumption of corn stover and electricity. Life cycle assessment (LCA) was used to evaluate primary fossil energy (PFE) depletion and greenhouse gas (GHG) emissions of this work (Fig. 7(b)). Interestingly, the life cycle assessment results reveal that the PFE depletion and GHG emissions are 20×10^3 MJ/t and −1.1 t CO_2 eq/t xylene, respectively, which were dramatically lower than those of petro-xylene. The life cycle PFE depletion and GHG emissions suggest the carbon-negative route for green aromatics production from an aqueous ABE mixture. This process shows great potential in reducing CO_2 emission, contributing to the low-carbon society.

4. Conclusion

In conclusion, a new strategy for sustainable aromatics has been developed. Aqueous oxygenate mixture obtained from fermentation could be converted to aromatics with 58% liquid yield and 86% selectivity in the liquid over Zn modified HZSM-5 catalyst. The tracking of reaction intermediates by *in situ* dual–beam FTIR reveals that the excellent catalytic activity was attributed to the synergistic catalysis of BAS and LAS under the reaction conditions with an appropriate ratio of BAS to LAS (1.6). An "olefin pool" reaction mechanism was proposed: acetone, butanol, and ethanol is deoxygenated to olefins via dehydration or decarbonylation, forming "olefin pool" and then to aromatization via oligomerization and dehydrogenation. Economic and environmental analysis suggests feasibility for selective conversion of aqueous ABE mixture to aromatics with a comparable cost of aromatics and −1.1 t greenhouse gas emissions per t xylene. It paves a green path for sustainable BTEX production from biomass-derived oxygenates which has a great potential industrial application.

CRediT authorship contribution statement

Yehong Wang: Investigation, Formal analysis, Writing – original draft, Writing – review & editing. **Jiaxu Liu:** Investigation, Formal analysis, Writing – original draft, Writing – review & editing. **Zhitong Zhao:** Investigation, Formal analysis, Writing – original draft, Writing – review & editing. **Qiang Guo:** Investigation, Formal analysis, Writing – review & editing. **Qike Jiang:** Investigation, Formal analysis. **Ning He:** Investigation, Formal analysis. **Feng Wang:** Conceptualization, Methodology, Writing – original draft, Writing – review & editing, Funding acquisition, Project administration.

Declaration of Competing Interest

The authors declare that they have no known competing financial interests or personal relationships that could have appeared to influence the work reported in this paper.

Data availability

All data are available from the corresponding author upon reasonable request.

Acknowledgements

This work supported by the National Natural Science Foundation of China (21972139, 21991094, 22025206, 21721004, U1862114, 21961130378), the "Strategic Priority Research Program of the Chinese Academy of Sciences" Grant No. XDB17000000, the Newton Advanced Fellowships (NAF\R1\191267) and DICP (DICP I201946).

Appendix A. Supporting information

Supplementary data associated with this article can be found in the online version at doi:10.1016/j.apcatb.2022.121139.

References

[1] J. Rockstrom, O. Gaffney, J. Rogelj, M. Meinshausen, N. Nakicenovic, H. J. Schellnhuber, A roadmap for rapid decarbonization, Science 355 (2017) 1269–1271, https://doi.org/10.1126/science.aah3443.
[2] R.F. Service, Clean revolution, Science 350 (2015) 1020–1023, https://doi.org/10.1126/science.350.6264.1020.
[3] K.S. Lackner, A guide to CO_2 sequestration, Science 300 (2003) 1677–1678, https://doi.org/10.1126/science.1079033.
[4] S. Mallapaty, How China could be carbon neutral by mid-century, Nature 586 (2020) 482–483, https://doi.org/10.1038/d41586-020-02927-9.
[5] M.R. Rahimpour, M. Jafari, D. Iranshahi, Progress in catalytic naphtha reforming process: a review, Appl. Energ. 109 (2013) 79–93, https://doi.org/10.1016/j.apenergy.2013.03.080.
[6] H.-G. Franck, J.W. Stadelhofer, Industrial Aromatic Chemistry, Springer, Heidelberg, 1988.
[7] Y.Z. Xiang, H. Wang, J.H. Cheng, J. Matsubu, Progress and prospects in catalytic ethane aromatization, Catal. Sci. Technol. 8 (2018) 1500–1516, https://doi.org/10.1039/c7cy01878a.
[8] W. Zhou, J.X. Liu, L. Lin, X.T. Zhang, N. He, C.Y. Liu, H.C. Guo, Enhanced dehydrogenative aromatization of propane by incorporating Fe and Pt into the Zn/HZSM-5 catalyst, Ind. Eng. Chem. Res. 57 (2018) 16246–16256, https://doi.org/10.1021/acs.iecr.8b03865.
[9] Z.L. Li, A.W. Lepore, M.F. Salazar, G.S. Foo, B.H. Davison, Z.L. Wu, C.K. Narula, Selective conversion of bio-derived ethanol to renewable BTX over Ga-ZSM-5, Green Chem. 19 (2017) 4344–4352, https://doi.org/10.1039/c7gc01188a.

[10] X.C. Chen, M. Dong, X.J. Niu, K. Wang, G. Chen, W.B. Fan, J.G. Wang, Z.F. Qin, Influence of Zn species in HZSM-5 on ethylene aromatization, Chin. J. Catal. 36 (2015) 880–888, https://doi.org/10.1016/S1872-2067(14)60289-8.
[11] S. He, I. Muizebelt, A. Heeres, N.J. Schenk, R. Blees, H.J. Heeres, Catalytic pyrolysis of crude glycerol over shaped ZSM-5/bentonite catalysts for Bio-BTX synthesis, Appl. Catal. B 235 (2018) 45–55, https://doi.org/10.1016/j.apcatb.2018.04.047.
[12] X.L. Yang, X. Su, D. Chen, T. Zhang, Y.Q. Huang, Direct conversion of syngas to aromatics: a review of recent studies, Chin. J. Catal. 41 (2020) 561–573, https://doi.org/10.1016/S1872-2067(19)63346-2.
[13] A. Kujawska, J. Kujawski, M. Bryjak, W. Kujawski, ABE fermentation products recovery methods- a review, Renew. Sustain. Energy Rev. 48 (2015) 648–661, https://doi.org/10.1016/j.rser.2015.04.028.
[14] H.P. Zhu, G.P. Liu, W.Q. Jin, Recent progress in separation membranes and their fermentation coupled processes for biobutanol recovery, Energy Fuel. 34 (2020) 11962–11975, https://doi.org/10.1021/acs.energyfuels.0c02680.
[15] P. Anbarasan, Z.C. Baer, S. Sreekumar, E. Gross, J.B. Binder, H.W. Blanch, D. S. Clark, F.D. Toste, Integration of chemical catalysis with extractive fermentation to produce fuels, Nature 491 (2012) 235–239, https://doi.org/10.1038/nature11594.
[16] B. Fridrich, M.C.A. Stuart, K. Barta, Selective coupling of bioderived aliphatic alcohols with acetone using hydrotalcite derived Mg-Al porous metal oxide and Raney nickel, ACS Sustain, ACS Sustain. Chem. Eng. 6 (2018) 8468–8475, https://doi.org/10.1021/acssuschemeng.8b00733.
[17] Y. Wang, M. Peng, J. Zhang, Z. Zhang, J. An, S. Du, H. An, F. Fan, X. Liu, P. Zhai, D. Ma, F. Wang, Selective production of phase-separable product from a mixture of biomass-derived aqueous oxygenates, Nat. Commun. 9 (2018) 5183, https://doi.org/10.1038/s41467-018-07593-0.
[18] A. Bhan, W.N. Delgass, Propane aromatization over HZSM-5 and Ga/HZSM-5 catalysts, Catal. Rev. Sci. Eng. 50 (2008) 19–151, https://doi.org/10.1080/01614940701804745.
[19] Z.Y. Chen, Y.M. Ni, Y.C. Zhi, F.L. Wen, Z.Q. Zhou, Y.X. Wei, W.L. Zhu, Z.M. Liu, Coupling of methanol and carbon monoxide over H-ZSM-5 to form aromatics, Angew. Chem. Int. Ed. 57 (2018) 12549–12553, https://doi.org/10.1002/anie.201807814.
[20] C.M. Lok, J. Van Doorn, G.A. Almansa, Promoted ZSM-5 catalysts for the production of bio-aromatics: a review, Renew. Sustain. Energy Rev. 113 (2019), 109248, https://doi.org/10.1016/j.rser.2019.109248.
[21] T. Ennaert, J. Van Aelst, J. Dijkmans, R. De Clercq, W. Schutyser, M. Dusselier, D. Verboekend, B.F. Sels, Potential and challenges of zeolite chemistry in the catalytic conversion of biomass, Chem. Soc. Rev. 45 (2016) 584–611, https://doi.org/10.1039/c5cs00859j.
[22] C.J. Liu, H.M. Wang, A.M. Karim, J.M. Sun, Y. Wang, Catalytic fast pyrolysis of lignocellulosic biomass, Chem. Soc. Rev. 43 (2014) 7594–7623, https://doi.org/10.1039/c3cs60414d.
[23] S.M.T. Almutairi, B. Mezari, P.C.M.M. Magusin, E.A. Pidko, E.J.M. Hensen, Structure and reactivity of Zn-modified ZSM-5 zeolites: the importance of clustered cationic Zn complexes, ACS Catal. 2 (2012) 71–83, https://doi.org/10.1021/cs200441e.
[24] K.C. Szeto, A. Gallo, S. Hernandez-Morejudo, U. Olsbye, A. De Mallmann, F. Lefebvre, R.M. Gauvin, L. Deevoye, S.L. Scott, M. Taoufik, Selective grafting of Ga(*i*-Bu)$_3$ on the silanols of mesoporous H-ZSM-5 by surface organometallic chemistry, J. Phys. Chem. C 119 (2015) 26611–26619, https://doi.org/10.1021/acs.jpcc.5b09289.
[25] Y.T. Cheng, J. Jae, J. Shi, W. Fan, G.W. Huber, Production of renewable aromatic compounds by catalytic fast pyrolysis of lignocellulosic biomass with bifunctional Ga/ZSM-5 catalysts, Angew. Chem. Int. Ed. 51 (2012) 1387–1390, https://doi.org/10.1002/anie.201107390.
[26] P.Y. Dapsens, C. Mondelli, J. Perez-Ramirez, Design of Lewis-acid centres in zeolitic matrices for the conversion of renewables, Chem. Soc. Rev. 44 (2015) 7025–7043, https://doi.org/10.1039/c5cs00028a.
[27] Y.W. Zhou, H. Thirumalai, S.K. Smith, K.H. Whitmire, J. Liu, A.I. Frenkel, L. C. Grabow, J.D. Rimer, Ethylene dehydroaromatization over Ga-ZSM-5 catalysts: nature and role of Gallium speciation, Angew. Chem. Int. Ed. 59 (2020) 19592–19601, https://doi.org/10.1002/anie.202007147.
[28] V. Balasundram, N. Ibrahim, R.M. Kasmani, R. Isha, M.K. Abd Hamid, H. Hasbullah, Catalytic upgrading of biomass-derived pyrolysis vapour over metal-modified HZSM-5 into BTX: a comprehensive review, Biomass Convers. Biorefin. (2020), https://doi.org/10.1007/s13399-020-00909-5.
[29] C.M. Lok, J. Van Doorn, G.A. Almansa, Promoted ZSM-5 catalysts for the production of bio-aromatics, a review, Renew. Sustain. Energy Rev. 113 (2019), 109248, https://doi.org/10.1016/j.rser.2019.109248.
[30] International Organization for Standardization, ISO14040 Environmental Management - Life Cycle Assessment - Principle and Framework, Geneva, 2006.
[31] J. Chen, Z.C. Feng, P.L. Ying, C. Li, ZnO clusters encapsulated inside micropores of zeolites studied by UV Raman and laser-induced luminescence spectroscopies, J. Phys. Chem. B 108 (2004) 12669–12676, https://doi.org/10.1021/jp048746x.
[32] H.Q. Wang, Y.L. Hou, W.J. Sun, Q.K. Hu, H. Xiong, T.F. Wang, B.H. Yan, W.Z. Qian, Insight into the effects of water on the ethene to aromatics reaction with HZSM-5, ACS Catal. 10 (2020) 5288–5298, https://doi.org/10.1021/acscatal.9b05552.
[33] J.B. Zhou, M.B. Gao, J.L. Zhang, W.J. Liu, T. Zhang, H. Li, Z.C. Xu, M. Ye, Z.M. Liu, Directed transforming of coke to active intermediates in methanol-to-olefins catalyst to boost light olefins selectivity, Nat. Commun. 12 (2021) 17, https://doi.org/10.1038/s41467-020-20193-1.
[34] H.F. Xiong, S. Lin, J. Goetze, P. Pletcher, H. Guo, L. Kovarik, K. Artyushkova, B. M. Weckhuysen, A.K. Datye, Thermally stable and regenerable platinum-tin clusters for propane dehydrogenation prepared by atom trapping on ceria, Angew. Chem.-Int. Ed. 56 (2017) 8986–8991, https://doi.org/10.1002/anie.201701115.
[35] Y.L. Shan, Z.J. Sui, Y. Zhu, D. Chen, X.G. Zhou, Effect of steam addition on the structure and activity of Pt-Sn catalysts in propane dehydrogenation, Chem. Eng. J. 278 (2015) 240–248, https://doi.org/10.1016/j.cej.2014.09.107.
[36] Y.L. Shan, Y.A. Zhu, Z.J. Sui, D. Chen, X.G. Zhou, Insights into the effects of steam on propane dehydrogenation over a Pt/Al2O3 catalyst, Catal. Sci. Technol. 5 (2015) 3991–4000, https://doi.org/10.1039/c5cy00230c.
[37] J.X. Liu, N. He, W. Zhou, L. Lin, G.D. Liu, C.Y. Liu, J.L. Wang, Q. Xin, G. Xiong, H. C. Guo, Isobutane Aromatization over a Complete Lewis Acid Zn/HZSM-5 Zeolite Catalyst: Performance and Mechanism, Catal. Sci. Technol. 8 (2018) 4018–4029, https://doi.org/10.1039/c8cy00917a.
[38] J.X. Liu, J.L. Wang, W. Zhou, C.L. Miao, G. Xiong, Q. Xin, H.C. Guo, Construction of an operando dual-beam fourier transform infrared spectrometer and its application in the observation of isobutene reactions over nano-sized HZSM-5 zeolite, Chin. J. Catal. 38 (2017) 13–19, https://doi.org/10.1016/S1872-2067(17)62751-7.